Supporting Information

Electrochemical Evidence for Hemilabile Coordination of 1,3-Dimethyllumazine to 1,1'-Bis(diorganophosphino)ferrocene-copper(I)

Rajkumar Jana,[a] Biprajit Sarkar,[b] Sabine Strobel,[a] Shaikh M. Mobin,[c] Wolfgang Kaim,[a,] Jan Fiedler[d,*]*

[a] Institut für Anorganische Chemie, Universität Stuttgart, Pfaffenwaldring 55, D-70550 Stuttgart, Germany

[b] Institut für Chemie und Biochemie, Freie Universität Berlin, Fabeckstraße 34-36, D- 14195 Berlin, Germany

[c] Discipline of Chemistry, School of Basic Sciences, Indian Institute of Technology Indore, Indore 452017, India

[d] J. Heyrovský Institute of Physical Chemistry, v.v.i., Academy of Sciences of the Czech Republic, Dolejškova 3, CZ-18223 Prague, Czech Republic

Table S1. Crystallographic data and refinement parameters for [Cu(dippf)(DML)](BF$_4$)×CH$_2$Cl$_2$

empirical formula	$C_{30}H_{44}BCuF_4FeN_4O_2P_2 \times CH_2Cl_2$
formula mass (g / mol)	845.76
T (K)	100 (2)
λ (Å)	0.71073, MoKα
crystal system	monoclinic
space group	$P2_1/n$
a (Å)	15.9608(3)
b (Å)	11.7770(2)
c (Å)	20.7616(4)
β (°)	110.998(1)
V (Å^3)	3643.41(12)
D_{calcd} (g/cm^3)	1.542
μ (mm^{-1})	1.272
crystal habit, color	coarse shape, red
crystal size (mm)	0.6 × 0.4 × 0.2
value of Z	4
θ range (°)	0.41-28.28
index ranges	$-21 \le h \le 21$, $-15 \le k \le 15$, $-27 \le l \le 27$
refl. collected	17116
refl. unique	8973
goodness of fit on F^2	1.009
$R1(I > 2\sigma(I))$	0.0412
wR2 (all data)	0.0957

$(\Delta\rho)_{max,}$ $(\Delta\rho)_{min}$	0.696 / -0.477

Table S2. Crystallographic data and refinement parameters for [Cu(dppf)(DML)](BF$_4$)

empirical formula	$C_{42}H_{36}BCuF_4FeN_4O_2P_2$
formula mass (g / mol)	896.89
T (K)	150(2)
λ (Å)	0.71073, MoKα
crystal system	triclinic
space group	$P\bar{1}$
a (Å)	12.157(1)
b (Å)	13.536(2)
c (Å)	13.605(2)
α (°)	76.514(10)
β (°)	70.315(10)
γ (°)	70.216(4)
V (Å^3)	1965.6(4)
D_{calcd} (g/cm^3)	1.515
μ (mm^{-1})	1.053
crystal habit, color	block, orange
crystal size (mm)	0.24 × 0.22 × 0.18
Z	2
θ range (°)	3.05-25.00
index ranges	$-14 \le h \le 14$, $-13 \le k \le 16$, $-16 \le l \le 16$
refl. collected	17772

refl. unique	4758
refl. observed	6902
goodness of fit on F^2	1.017
$R1(I > 2\sigma(I))$	0.0669
wR2 (all data)	0.1365
$(\Delta\rho)_{max}$, $(\Delta\rho)_{min}$	0.786 / -0.507

Table S3. Parameters[a] from cyclic voltammetry simulation and experimental data fitting

Reaction [b]	[**1**]PF_6	[**2**]BF_4
A + e ⇔ C	E_0 = -1.39 V, $k_s = 10^4$ cm s^{-1}	E_0 = -1.34 V, $k_s = 10^4$ cm s^{-1}
B + e ⇔ D	E_0 = -1.87 V, k_s = 0.1 cm s^{-1}	E_0 = -1.81 V, $k_s = 4x10^{-3}$ cm s^{-1}
A ⇔ B	$k_f = 10^{-3}$ s^{-1}, $k_b = 1.1x10^{-2}$ s^{-1}	$k_f = 10^{-3}$ s^{-1}, $k_b = 1.7x10^{-3}$ s^{-1}
C ⇔ D	$k_f = 10^{-11}$ s^{-1}, $k_b = 1.4x10^{-2}$ s^{-1}	$k_f = 7x10^{-9}$ s^{-1}, k_b = 1.02 s^{-1}
C → E + F	k = 0.13 s^{-1}	k = 0.35 s^{-1}
D → E + F	k = 0.01 s^{-1}	k = 0.01 s^{-1}

[a] E_0 = standard redox potential, k_s = heterogeneous charge-transfer rate constant, k = rate constant of homogeneous chemical reaction (k_f - forward, k_b – backward). [b] General reaction scheme derived from the reduction mechanism in Scheme 2.

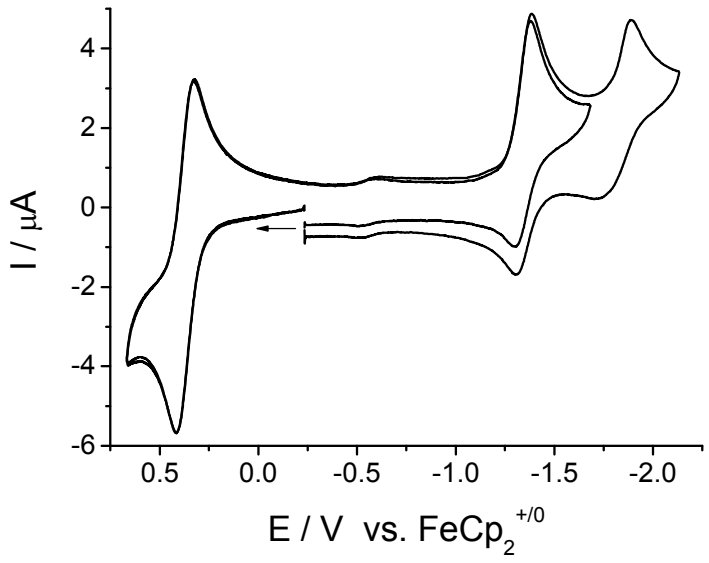

Figure S1. Cyclic voltammetry of [**2**]BF_4 in CH_2Cl_2/0.1M Bu_4NBF_4 at a glassy carbon electrode, scan rate 200 mV/s.

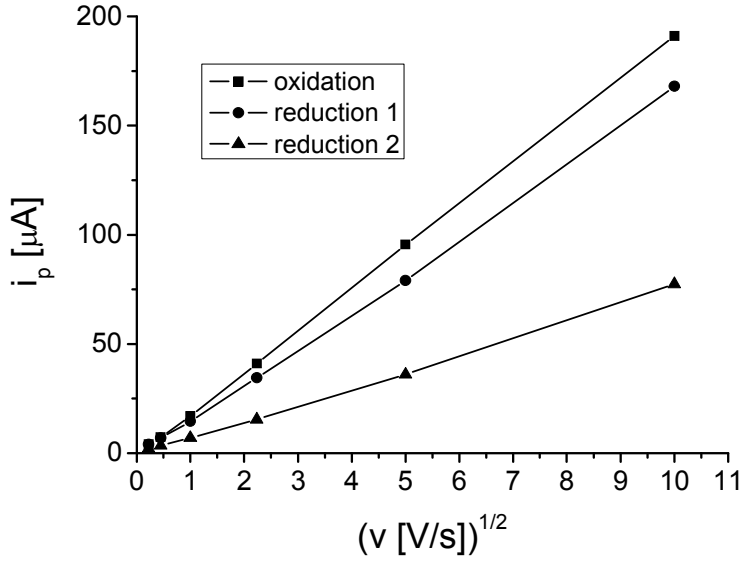

Figure S2. Dependence of peak intensities on the scan rate from cyclic voltammetry of [**1**]PF_6 in CH_2Cl_2/0.1M Bu_4NPF_6.

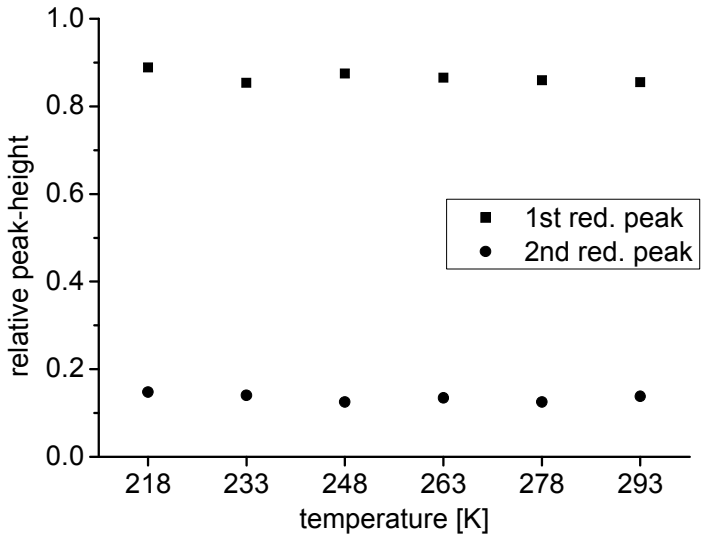

Figure S3. Temperature dependence of the reduction peak heights relative to the height of the anodic oxidation peak (dopf ferrocene) from cyclic voltammetry of [**1**]PF_6 in CH_2Cl_2/0.1 M Bu_4NPF_6 at 100 mV/s.

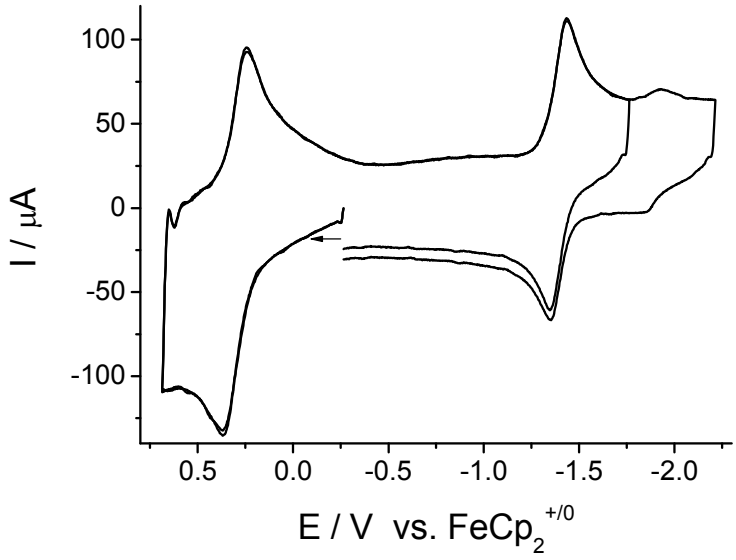

Figure S4. Cyclic voltammetry of [**1**]PF_6 in CH_2Cl_2 / 0.1 M Bu_4NPF_6 at a glassy carbon electrode, scan rate 25 V/s.

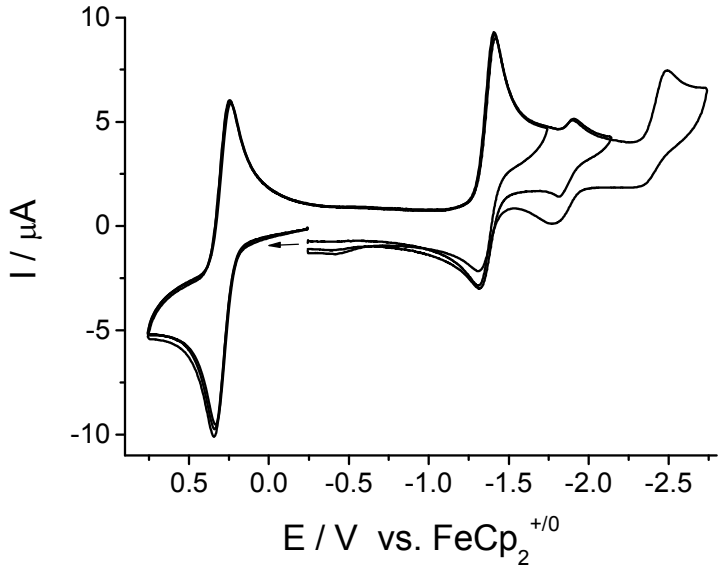

Figure S5. Cyclic voltammetry of [**1**]PF_6 in in acetone/0.1 M Bu_4NPF_6 at a glassy carbon electrode, scan rate 200 mV/s.

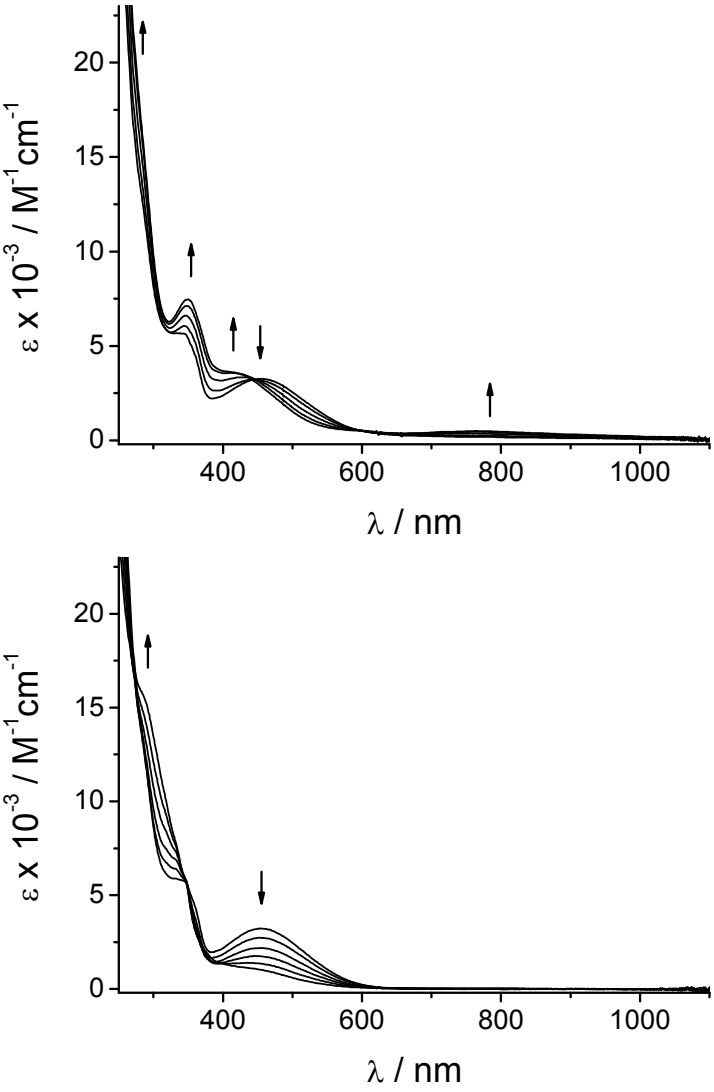

Figure S6. UV-Vis spectroelectrochemical change during oxidation (top) an reduction (bottom) of [**2**]PF_6 in CH_2Cl_2/0.1 M Bu_4NPF_6.

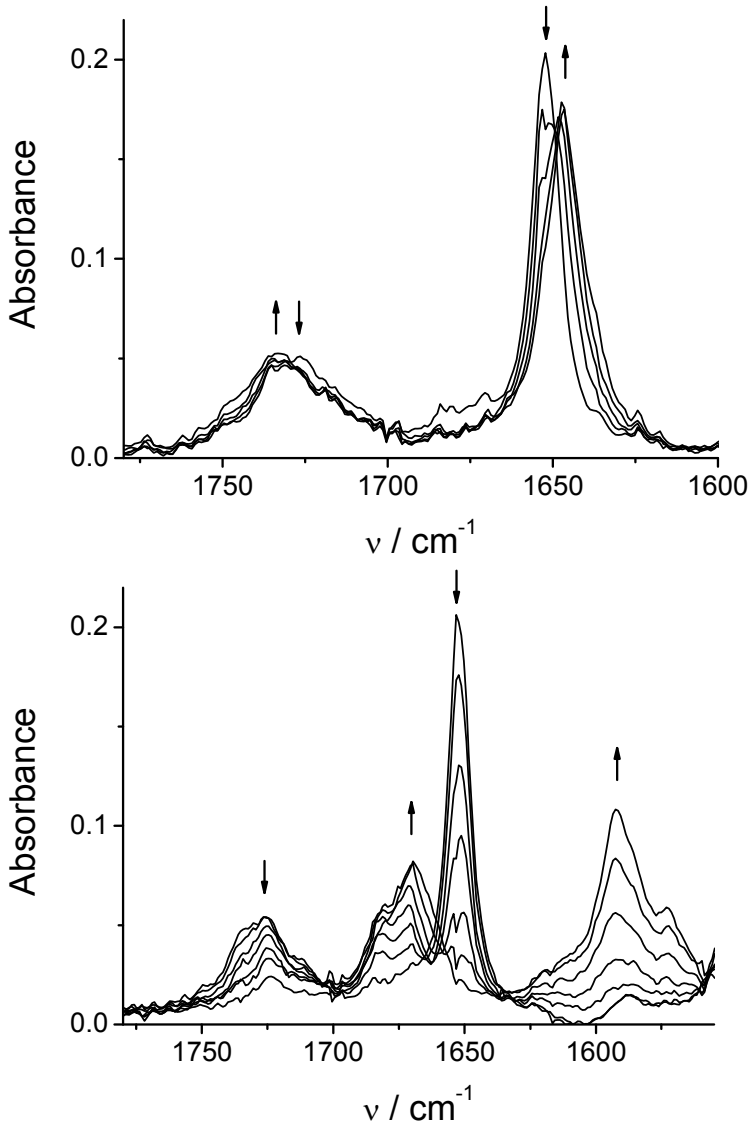

Figure S7. IR spectroelectrochemical change during oxidation (top) and reduction (bottom) of [**2**]PF_6 in CH_2Cl_2/0.1 M Bu_4NPF_6.

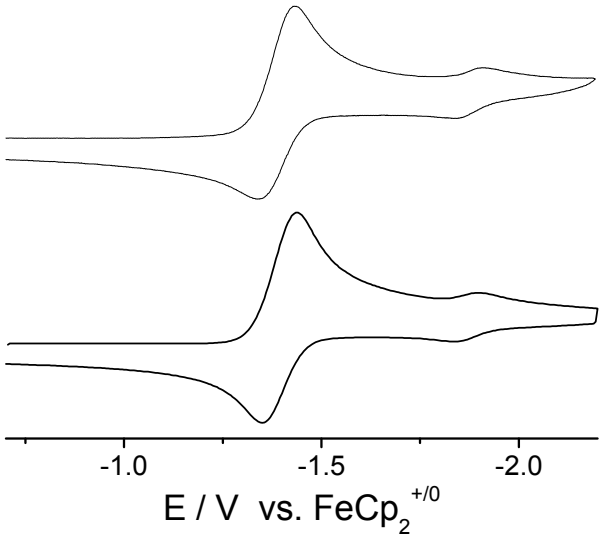

Figure S8. Experimental cyclic voltammogram (top) of [**1**]PF_6 in CH_2Cl_2/0.1M Bu_4NPF_6, scan rate 200 mV/s, and voltammogram simulated using parameters from Table S3 (bottom).

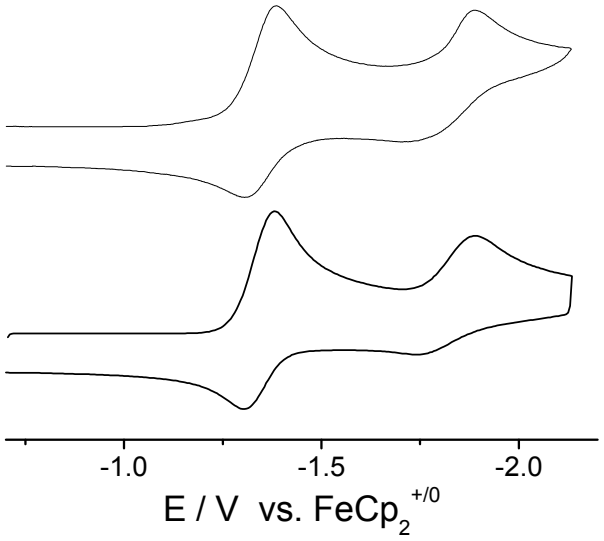

Figure S9. Experimental cyclic voltammogram (top) of [**2**]BF_4 in CH_2Cl_2/0.1M Bu_4NBF_4, scan rate 200 mV/s, and voltammogram simulated using parameters from Table S3 (bottom).